IEIE Transactions on Smart Processing and Computing, vol. 4, no. 4, August 2015
http://dx.doi.org/10.5573/IEIESPC.2015.4.4.272

Construction of Confusion Lines for Color Vision Deficiency and Verification by Ishihara Chart

Keuyhong Cho, Jusun Lee, Sanghoon Song, and Dongil Han*

Department of Computer Engineering, Sejong University
isolat09@naver.com, jusunleeme@nate.com, song@sejong.ac.kr, dihan@sejong.ac.kr

***** Corresponding Author: Author: Dongil Han

Received June 20, 2015; Revised July 15, 2015; Accepted August 24, 2015; Published August 31, 2015

** Regular Paper*

***Abstract*:** This paper proposes color databases that can be used for various purposes for people with a color vision deficiency (CVD). The purpose of this paper is to group colors within the sRGB gamut into the CIE L*a*b* color space using the Brettel algorithm to simulate the representative colors of each group into colors visible to people with a CVD, and to establish a confusion line database by comparing colors that might cause confusion for people with different types of color vision deficiency. The validity of the established confusion lines were verified by using an Ishihara chart. The different colors that confuse those with a CVD in an Ishihara chart are located in the same confusion line database for both protanopia and deutanopia. Instead of the 3D RGB color space, we have grouped confusion colors to the CIE L*a*b* space coordinates in a more distinctive and intuitive manner, and can establish a database of colors that can be perceived by people with a CVD more accurately. Editor - Highlight - Do these changes reflect the intended meaning? If not, please rephrase as intended.

***Keywords*:** Color vision deficiency, Ishihara chart, Confusion line, Color vision deficiency simulation

1. Introduction

The recent remarkable developments in display technology have ushered in an environment where color information display devices are ubiquitous, and where people can enjoy more color information than at any time in history. Although about 92% of the world's people can enjoy the benefits of rich color, for the remaining 8% who have a color vision deficiency (CVD), it is not possible. People with a CVD are usually classified into three groups: protan (red color-blind), deutan (green color-blind), and tritan (blue color-blind). The protan population has abnormal L-cone cells, which are sensitive to red light, whereas the deutan population has abnormal M-cone cells, which perceive green; both types account for approximately 95% of the people with a CVD. The remaining 5%, a small percentage, belong to the tritan group, characterized by an absence of the S-cone cells sensitive to blue light [1].

In this paper, we proposed an algorithm to construct a database of confusion lines in order to identify colors that cause confusion for people with a CVD. To solve the problem, we used the protanopia and deuteranopia simulation [2, 3, 4] algorithms proposed by Brettel to construct a database of confusion lines within the sRGB gamut, but in the CIE L*a*b* color space [5]. However, because the definition of color differences within the sRGB color gamut is ambiguous, we selected the representative values from the sRGB color gamut in the CIE L*a*b* color space, which is more similar to real color perception in humans, in order to produce more effective results. By using colors that are grouped according to different types of CVD, we could establish a database of confusion lines that cause confusion for people with each type of CVD.

2. Related Work

Some previous research [6] proposed a way of changing colors from the color pallet that cause confusion for people with a CVD in order to prevent that confusion, and other research [7, 8] proposed establishing a database of confusion lines by using the sRGB color space. But this

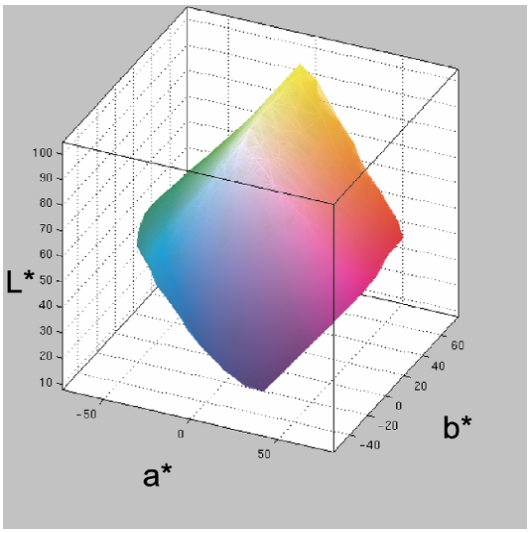

Fig. 1. sRGB color gamut in the CIE L*a*b* color space.

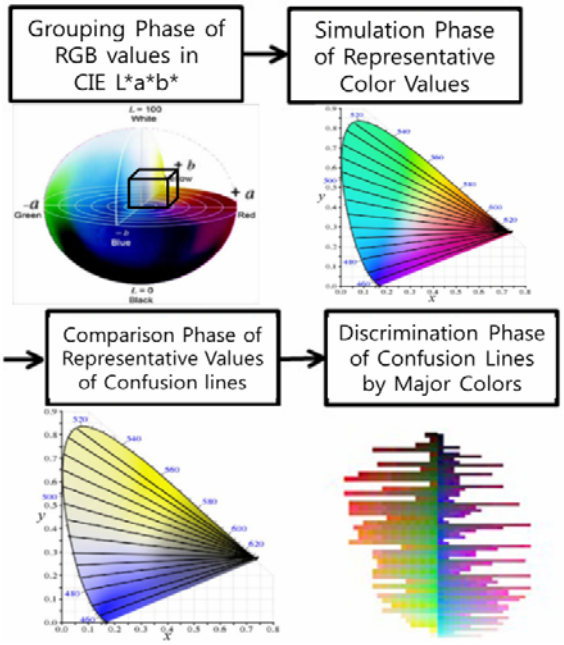

Fig. 2. These figures showed the four steps of a confusion line database construction procedure.

previous research did not consider the characteristics of human color perception. As a result, some color data might be lost in the process of grouping representative values. Given this, we used colors within the sRGB gamut in the CIE L*a*b* color space to reflect the features of human color perception, and that color gamut is shown in Fig. 1 [9].

3. The Proposed Scheme

Fig. 2 diagrams how to construct a confusion line database (DB) proposed by this research. In the preliminary phase, we created color boxes in the CIE L*a*b* color space by grouping RGB color values to CIE L*a*b* coordinates, and selected their central points as their representative values. We selected the representative values and simulated them by using the protanopia and deutanopia simulation algorithms proposed by Brettel and constructed a database of confusion lines based on the given conditions by comparing the simulated representative values.

3.1 Grouping Phase of RGB values in CIE L*a*b*

The gamut of the CIE L*a*b* color space [10] is L^* : $0 \sim 100$, a^* : $-128 \sim 128$, b^* : $-128 \sim 128$. This phase groups all $L^*a^*b^*$ color values to the CIE L*a*b* 3D color coordinates. In the CIE L*a*b* color space, five units in L^* are grouped together, while 13 units in each of a^* and b^* are grouped together. Therefore, virtual boxes such as L^*_{box}, a^*_{box} and b^*_{box} were created by dividing L^*, a^* and b^*, respectively, into 20 equal parts. We can create these virtual boxes by using Eqs. (1) to (3). Although the number of virtual boxes in the CIE L*a*b* color space can be 8,000 (20x20x20), we removed colors that exist in the CIE L*a*b* color space but not in the sRGB space. The total number of virtual boxes used by this research is 982. After creating virtual boxes from (0, 0, -2) to (19, -2, 5), we calculated the central points of the virtual boxes by using Eqs. (4) to (6), and then assigned the representative values of L^*_{pri}, a^*_{pri} and b^*_{pri} to their respective virtual boxes.

$$L^*_{box} = (L^*/5); \quad (1)$$

$$a^*_{box} = (a^*/13); \quad (2)$$

$$b^*_{box} = (b^*/13); \quad (3)$$

$$L^*_{pri} = L^*_{box} + 2.5; \quad (4)$$

$$a^*_{pri} = a^*_{box} + 6.5; \quad (5)$$

$$b^*_{pri} = b^*_{box} + 6.5; \quad (6)$$

3.2 Simulation Phase of Representative Color Values

In the simulation phase of representative color values, we conducted the simulation of color appearance by comparing the representative color value of the central point of a rectangular L*a*b* virtual box, which was created in the RGB value grouping process, to the CIE L*a*b* space. We also implemented the protanopia and deutanopia simulation algorithms proposed by Vienot et al. [2]. Fig. 3 shows the confusion lines of protanopia in a CIE 1931 chromaticity diagram and the simulation image perceived by someone with protanopia.

3.3 Comparison Phase of Representative Values of Confusion Lines

The representative values of the existing confusion lines were calculated using Eqs. (4) to (6). Eq. (7) calculates the color difference between (L^*_1, a^*_1, b^*_1) and

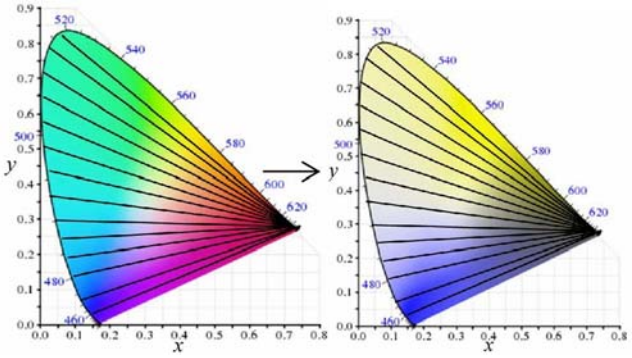

Fig. 3. Before and after Brettel color simulation in a CIE 1931 chromaticity diagram.

$\left(L_2^*, a_2^*, b_2^*\right)$ in CIE L*a*b* space. If condition (8) is met, each representative color pair, which looked different before color simulation, looks like the same color after the simulation. And this color pair causes confusion to people who have a CVD, but not to people who do not. In addition, whenever a color is added to a confusion line, the representative values $PL^*_{(x)}$, $Pa^*_{(x)}$, $Pb^*_{(x)}$ of each confusion line were recalculated using Eqs. (9) - (11) to provide a more reliable algorithm to construct a database of confusion lines.

A conventional color difference equation uses equation (12), which was used to calculate the existing color differences [10, 11] with two color pairs: (L_1^*, a_1^*, b_1^*), (L_2^*, a_2^*, b_2^*). There are some cases where people with a CVD can distinguish similar colors, depending on the level of brightness. To avoid this, we used condition (8) instead of condition (12).

$$\Delta L^* = L_1^* - L_2^*$$

$$\Delta a b^* = \sqrt{(a_1^* - a_2^{*\,2} + b_1^* - b_2^{*\,2}} \quad (7)$$

$$\Delta L^* <= 3 \text{ and } \Delta a b^* <= 15 \quad (8)$$

$$PL^*_{(x)} = \frac{1}{n_x} \cdot \sum_{i=0}^{n_x} L^*_i \quad (9)$$

$$Pa^*_{(x)} = \frac{1}{n_x} \cdot \sum_{i=0}^{n_x} a^*_i \quad (10)$$

$$Pb^*_{(x)} = \frac{1}{n_x} \cdot \sum_{i=0}^{n_x} b^*_i \quad (11)$$

$$\Delta E^* = \sqrt{(a_1^* - a_2^{*\,2} + b_1^* - b_2^{*\,2} + L_1^* - L_2^{*\,2}} \quad (12)$$

Blue :

$$\varphi >= 270^o \,||\, \varphi <= 90^o$$

Yellow :

$$\varphi < 270^o \,\&\&\, \varphi > 90^o \quad (13)$$

where φ is the azimuth angle component in a spherical coordinate system

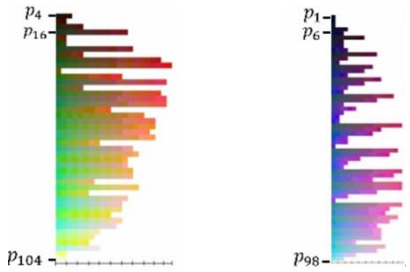

(a) Yellow confusion line group (b) Blue confusion line group

Fig. 4. Yellow confusion line group and blue confusion line group for people with protanopia.

3.4 Discrimination Phase of Confusion Lines by Major Colors

When we looked into the simulated color DB after we finished the the construction of confusion lines using the algorithm proposed by this research, the simulated colors were divided into two dominant colors. The major colors that can be perceived by people with protanopia or deutanopia are divided into yellow and blue regions. In this research, we classified each confusion line either into the yellow DB or into the blue DB. By dividing the confusion line DB by major colors, confusing colors can be clearly distinguished. Given this, we converted the coordinates in the CIE L*a*b* color space into spherical coordinates, and distinguished confusion lines by major colors using condition (13) [12], which was designed to discriminate colors using angle φ in order to make color compensation more useful for people with a CVD. The result of this algorithm is shown in Fig. 4. The X-axis represents the number of colors in each confusion line, and the y-axis represents the confusion line type in both groups.

4. Experimental Results

To verify the confusion lines created based on the algorithm proposed by this research, we compared them with the existing confusion lines. Fig. 5(a) shows the theoretical confusion lines for people with protanopia. Fig. 5(b) shows the generated confusion lines from using the proposed algorithm. The theoretical confusion lines ignore brightness. Thus, the colors on the same confusion lines can be differentiated by someone with protanopia because of the difference in brightness. But the confusion lines established by the suggested algorithm can distinguish brightness, thus creating more effective confusion lines. Fig. 6 shows the generated confusion lines by using the proposed algorithm in the CIE L*a*b* color space. Fig. 7 shows all confusion lines for those with protanopia and deutanopia. The vertical axis indicates the number of confusion lines for people with each type of CVD, while the horizontal axis shows the different colors that exist on the same confusion line. For example, Fig. 7(c) lists the representative color values of each confusion line for people with deutanopia. We can see that red and green

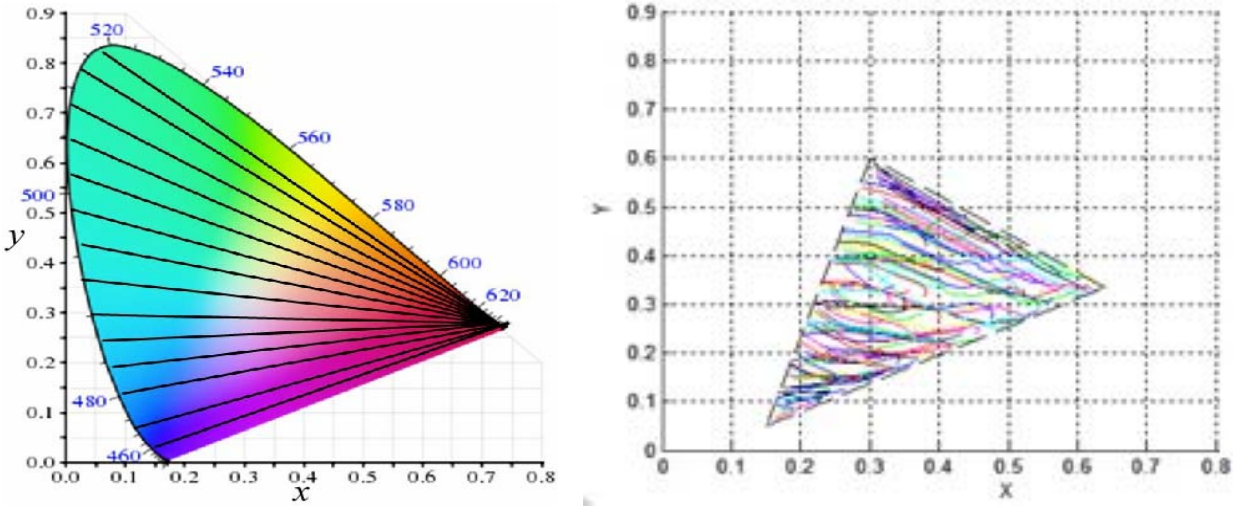

(a) Confusion lines in the CIE xy color space [5] (b) Proposed confusion lines

Fig. 5. Proposed confusion lines for people with protanopia within the CIE xy color space.

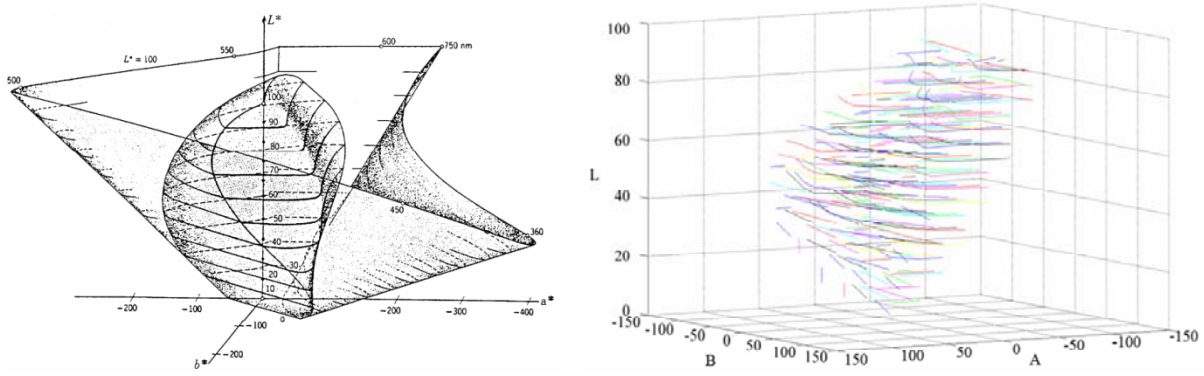

(a) CIE L*a*b* color space (b) Proposed confusion lines

Fig. 6. Proposed confusion lines for people with protanopia within the CIE L*a*b* color space.

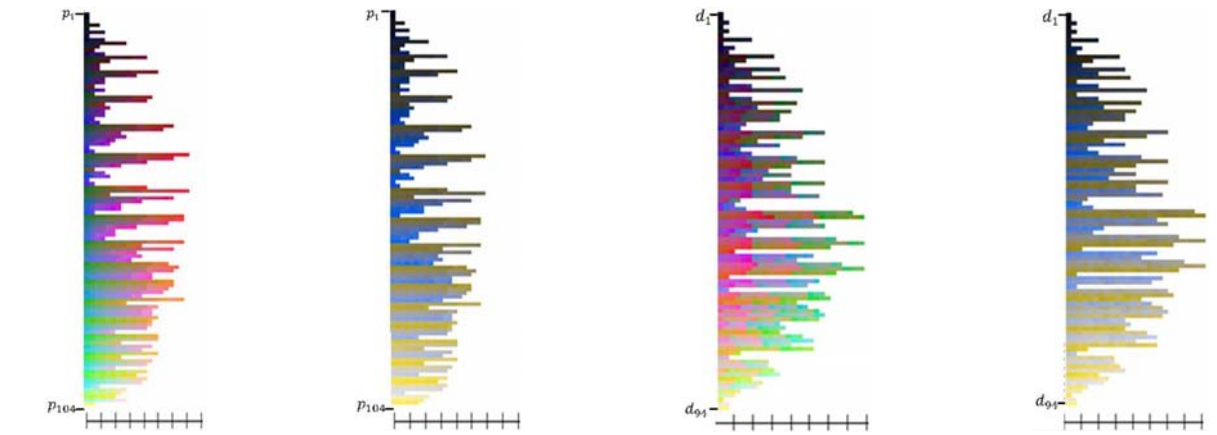

(a) Protanopia confusion lines (104 lines)

(b) Simulation image (a) perceived by someone with protanopia

(c) Deutanopia confusion lines (94 lines)

(d) Simulation image (c) perceived by someone with deutanopia

Fig. 7. Arrangement of representative colors for created confusion lines.

exist on the same confusion lines. Because each CVD patient can discern similar colors depending on brightness, we can see that they do not exist on the same horizontal axis in Fig. 7(c). For Fig. 7(a), the results are the same. Fig. 8 shows three confusion lines, which were magnified to help explain Fig. 7. After the construction of confusion

(a) Deutanopia confusion lines in D60, D61, and D62

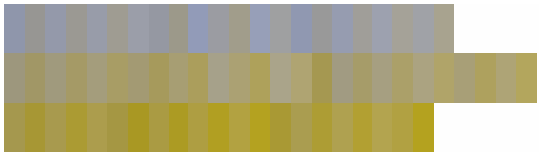

(b) Simulation image (a) perceived by someone with deutanopia

Fig. 8. Magnified images of arrangement of representative colors.

Table 1. Constructed Confusion Lines.

Deficiency	Confusion Lines	Confusion Boxes
Protanopia	P1 … P27 … P104	(0 0 -2) … (5 3 -6) (5 4 -7) (5 4 -6) … (19 -1 0), (19 -1 1)
Deuteranopia	D1 … D27 … D95	(0 0 -2) … (5 3 -4) (6 0 -3) (6 1 -4) (6 2 -4) (6 2 -3) … (19 -1 0), (19 -1 1)

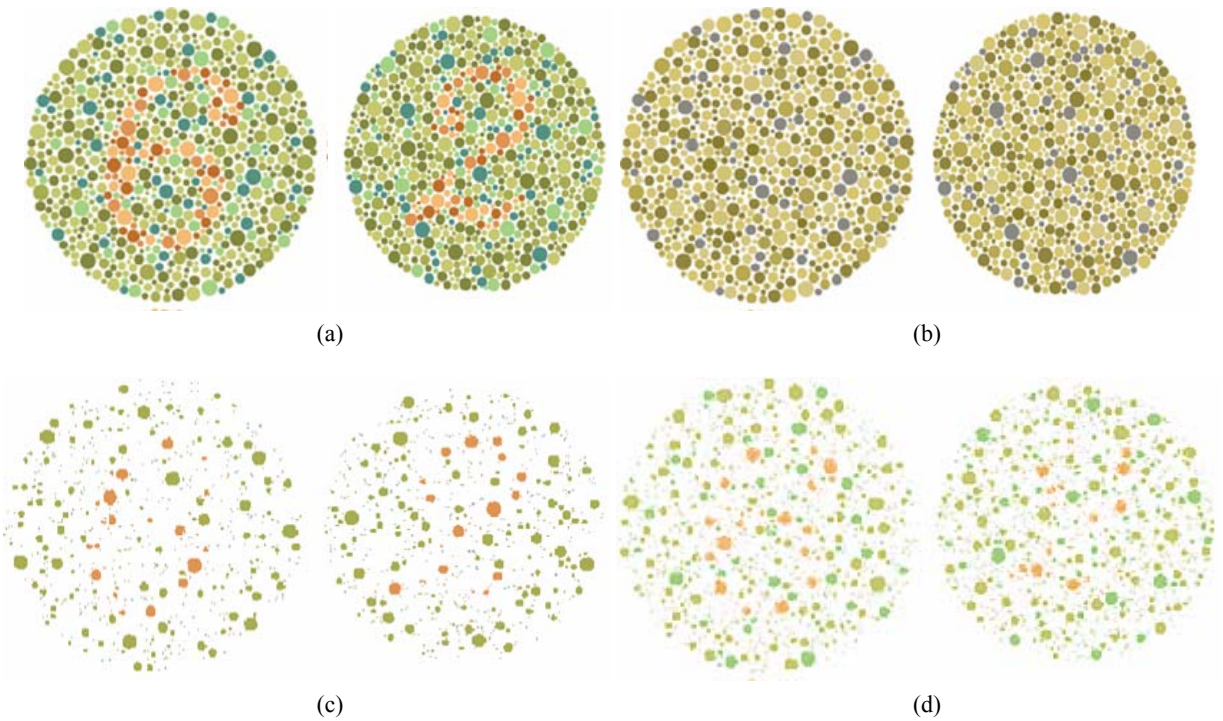

(a) (b) (c) (d)

(a) Ishihara chart perceived by people without a CVD; (b) Ishihara chart perceived by people with a CVD;
(c) colors on the P14 confusion line within an Ishihara chart, and (d) colors on the P17 confusion line within an Ishihara chart.

Fig. 9. Ishihara chart test results.

lines for people with protanopia or deutanopia, we found that the number of confusion lines for those with protanopia amounted to 104, ranging from P1 to P104, while the number for those with deutanopia was 95, ranging from D1 to D95, as shown in Table 1.

To verify these results, we classified colors based on the databases of confusion lines created in an Ishihara chart. We checked how confusion lines were distributed by analyzing colors within an Ishihara chart using the confusion line DB. As shown in Fig. 9(a), numbers 6 and 2 are visible for people without a CVD. Other examples are Figs. 9(c) and (d). Figs. 9(c) and (d) show the colors that exist on the P14 confusion line and the P17 confusion line, respectively, within each Ishihara chart. As seen below, we found that the color for numbers 6 and 2 in the Ishihara chart and the background colors exist on the same confusion lines. Therefore, people with a CVD could not see the numbers within Ishihara charts like Fig. 9(b).

5. Conclusion

Previous research was conducted by grouping confusion colors in the 3D RGB color space, and some color data might be lost in the grouping process. However, if we use the confusion line construction method proposed by this research, we can group confusion colors on the CIE L*a*b* color space coordinates in a more distinctive and intuitive manner and can establish a database of colors that can be perceived by people with a CVD in a more accurate

manner. Therefore, we were able to group a wider color range and more varied colors that can be perceived by people with a CVD than the existing confusion line databases. The generated confusion line DB for protanopia and deutanopia will contribute greatly to the development of other research on people with a CVD.

Acknowledgement

This work was supported by a National Research Foundation of Korea grant funded by the Korean Government (NRF-2014R1A1A2058592), and was also supported by a National Research Foundation of Korea grant funded by the Korean Government (No. 2012-007498).

References

[1] M. P. Simunovic, "Colour vision deficiency," Eye, 24.5, pp. 747-755, 2009. Article (CrossRef Link)
[2] F. Vienot, H. Brettel, J. D. Mollon, "Digital Video Colourmaps for Checking the Legibility of Displays by Dichromats," Color Research and Application, 24.4, pp. 243-252, August, 1999. Article (CrossRef Link)
[3] G. M. Machado, et al., "A physiologically-based model for simulation of color vision deficiency," Visualization and Computer Graphics, IEEE Transactions on 15.6, pp. 1291-1298, 2009. Article (CrossRef Link)
[4] C. Rigden, "'The Eye of the Beholder'-Designing for Colour-Blind Users," British Telecommunications Engineering 17, pp. 291-295, 1999. Article (CrossRef Link)
[5] CIE ColorSpace. [Online]. Available: Article (CrossRef Link)
[6] D. Han, S. Yoo and B. Kim, "A Novel Confusion-Line Separation Algorithm Based on Color Segmentation for Color Vision Deficiency," Journal of Imaging Science & Technology, 56.3, 2012. Article (CrossRef Link)
[7] S. Park, Y. Kim, "The Confusing Color line of the Color deficiency in Panel D-15 using CIELab Color Space" Journal of Korean Ophthalmic Optics Society 6 pp. 139-144, 2001 Article (CrossRef Link)
[8] P. Doliotis, et al., "Intelligent modification of colors in digitized paintings for enhancing the visual perception of color-blind viewers," Artificial Intelligence Applications and Innovations III, pp. 293-301, 2009. Article (CrossRef Link)
[9] CIE 1931. [Online].Available: Article (CrossRef Link)
[10] CIE. Technical report: Industrial colour-difference evaluation. CIE Pub. No. 116. Vienna: Central Bureau of the CIE; 1995. Article (CrossRef Link)
[11] Manuel Melgosa, "Testing CIELAB-based color-difference formulas," Color Research & Application, 25.1, pp. 49-55, 2000. Article (CrossRef Link)
[12] H. Brettel, F. Viénot, and J. D. Mollon. "Compu-terized simulation of color appearance for dichromats," JOSA A, 14.10, pp. 2647-2655, 1997. Article (CrossRef Link)

Appendix

See Table 2

Table 2. Confusion line map for protanopin

Type of confusion line	Box positions on same confusion line (L^* a^* b^*)
P1	(0 0 -2)
P2	(0 0 -1)
P3	(1 -1 -1)
P4	(1 -1 0), (1 0 0), (1 1 0)
P5	(1 0 -2), (1 0 -1), (1 1 -2), (1 1 -1)
P6	(1 1 -3), (1 2 -4), (1 2 -3)
P7	(2 -1 -1), (2 -1 0), (2 0 -1), (2 0 0), (2 1 -1), (2 1 0), (2 2 -1), (2 2 0)
P8	(2 0 -2), (2 1 -2), (2 2 -2)
P9	(2 1 -3), (2 2 -4), (2 2 -3)
P10	(2 1 1), (2 2 1)
P11	(2 3 -5), (3 2 -4), (3 3 -5), (3 3 -4)
P12	(3 -2 0), (3 -1 -1), (3 -1 0), (3 0 -1), (3 0 0), (3 1 -1), (3 1 0), (3 2 -1), (3 2 0), (4 3 -1), (4 3 0)
P13	(3 -2 1), (3 -1 1), (3 0 1), (3 1 1), (3 2 1)
P14	(3 0 -2), (3 1 -2), (3 2 -2), (4 3 -2)
P15	(3 1 -3), (3 2 -3)
P16	(4 -2 0), (4 -2 1), (4 -1 0), (4 -1 1), (4 0 0), (4 0 1), (4 1 0), (4 1 1), (4 2 0), (4 2 1), (5 3 0), (5 3 1),(5 3 2)
P17	(4 -1 -2), (4 -1 -1), (4 0 -2), (4 0 -1), (4 1 -2), (4 1 -1), (4 2 -2), (4 2 -1), (5 3 -2), (5 3 -1)

P18	(4 0 -3), (4 1 -4), (4 1 -3), (4 2 -4), (4 2 -3), (4 3 -4), (4 3 -3), (5 3 -3)
P19	(4 1 2), (4 2 2)
P20	(4 2 -5), (4 3 -5), (4 4 -6), (5 4 -5)
P21	(5 -3 2), (5 -2 2)
P22	(5 -2 0), (5 -2 1), (5 -1 0), (5 -1 1), (5 0 0), (5 0 1), (5 1 0), (5 1 1), (5 2 0), (5 2 1), (5 2 2), (6 3 0), (6 3 1), (6 3 2)
P23	(5 -1 -2), (5 -1 -1), (5 0 -2), (5 0 -1), (5 1 -2), (5 1 -1), (5 2 -2), (5 2 -1), (6 3 -2), (6 3 -1), (6 4 -2), (6 4 -1)
P24	(5 -1 2), (5 0 2), (5 1 2), (6 2 2), (6 3 3)
P25	(5 0 -3), (5 1 -4), (5 1 -3), (5 2 -4), (5 2 -3), (5 3 -4), (6 4 -4), (6 4 -3)
P26	(5 2 -5), (5 3 -5), (6 3 -4), (6 4 -5)
P27	(5 3 -6), (5 4 -7), (5 4 -6)
P28	(6 -3 1), (6 -3 2), (6 -2 1), (6 -2 2), (6 -1 1), (6 -1 2), (6 0 1), (6 0 2), (6 1 1), (6 1 2), (6 2 1), (7 2 1), (7 2 2), (7 2 3), (7 3 1), (7 3 2), (7 3 3), (7 4 2), (7 4 3)
P29	(6 -2 -1), (6 -2 0), (6 -1 -1), (6 -1 0), (6 0 -1), (6 0 0), (6 1 -1), (6 1 0), (6 2 -1), (6 2 0), (7 3 -1), (7 3 0), (7 4 -1), (7 4 0), (7 4 1)
P30	(6 -1 -2), (6 0 -3), (6 0 -2), (6 1 -3), (6 1 -2), (6 2 -3), (6 2 -2), (6 3 -3), (7 3 -2), (7 4 -3), (7 4 -2)
P31	(6 1 -4), (6 2 -4), (7 4 -4)
P32	(6 2 -5), (6 3 -5), (7 3 -4), (7 4 -5), (7 5 -5), (8 5 -4)
P33	(6 3 -6), (6 4 -6), (7 5 -6)
P34	(6 4 -7), (6 5 -7)
P35	(6 5 -8), (7 5 -7)
P36	(7 -3 1), (7 -3 2), (7 -2 1), (7 -2 2), (7 -1 1), (7 -1 2), (7 0 1), (7 0 2), (7 1 1), (7 1 2), (7 1 3), (8 2 1), (8 2 2), (8 2 3), (8 3 2), (8 3 3), (8 4 2), (8 4 3), (9 5 2), (9 5 3), (9 5 4)
P37	(7 -2 -1), (7 -2 0), (7 -1 -1), (7 -1 0), (7 0 -1), (7 0 0), (7 1 -1), (7 1 0), (7 2 -1), (7 2 0), (8 3 -1), (8 3 0), (8 3 1), (8 4 0), (8 4 1),(9 5 0), (9 5 1)
P38	(7 -1 -2), (7 0 -3), (7 0 -2), (7 1 -3), (7 1 -2), (7 2 -3), (7 2 -2), (7 3 -3), (8 4 -3), (8 4 -2), (8 4 -1), (8 5 -2)
P39	(7 0 -4), (7 1 -5), (7 1 -4), (7 2 -5), (7 2 -4), (7 3 -5), (8 4 -5), (8 4 -4), (8 5 -5), (8 5 -3)
P40	(7 0 3)
P41	(7 2 -6), (7 3 -6), (7 4 -6), (8 5 -6)
P42	(7 4 -7), (8 4 -6), (8 5 -7), (9 6 -6)
P43	(7 5 -8)
P44	(8 -4 3), (8 -3 3), (8 -2 3), (8 -1 3), (8 0 3), (8 1 3), (9 2 3), (9 3 3), (9 4 3), (9 4 4), (10 5 3), (10 5 4)
P45	(8 -3 0), (8 -3 1), (8 -2 0), (8 -2 1), (8 -1 0), (8 -1 1), (8 0 0), (8 0 1), (8 1 0), (8 1 1), (8 2 0), (9 2 1), (9 2 2), (9 3 0), (9 3 1), (9 3 2), (9 4 1), (9 4 2), (10 5 1), (10 5 2)
P46	(8 -3 2), (8 -2 2), (8 -1 2), (8 0 2), (8 1 2)
P47	(8 -2 -1), (8 -1 -2), (8 -1 -1), (8 0 -2), (8 0 -1), (8 1 -2), (8 1 -1), (8 2 -2), (8 2 -1), (8 3 -2), (9 3 -2), (9 3 -1), (9 4 -2), (9 4 -1), (9 4 0), (9 5 -1)
P48	(8 -1 -3), (8 0 -4), (8 0 -3), (8 1 -4), (8 1 -3), (8 2 -4), (8 2 -3), (8 3 -4), (8 3 -3), (9 4 -4), (9 4 -3), (9 5 -3), (9 5 -2), (10 6 -3)
P49	(8 1 -5), (8 2 -5), (8 3 -5), (9 4 -5), (9 5 -5), (9 5 -4), (10 6 -4)
P50	(8 2 -6), (8 3 -6), (9 5 -6), (10 6 -5)
P51	(8 3 -7), (8 4 -7), (9 4 -6)
P52	(9 -4 2), (9 -4 3), (9 -3 2), (9 -3 3), (9 -2 2), (9 -2 3), (9 -1 2), (9 -1 3), (9 0 2), (9 0 3), (9 1 2), (9 1 3), (10 2 2), (10 2 3), (10 2 4), (10 3 3), (10 3 4), (10 4 3), (10 4 4)
P53	(9 -3 0), (9 -3 1), (9 -2 0), (9 -2 1), (9 -1 0), (9 -1 1), (9 0 0), (9 0 1), (9 1 0), (9 1 1), (9 2 0), (10 2 0), (10 2 1), (10 3 0), (10 3 1), (10 3 2), (10 4 1), (10 4 2), (11 5 1), (11 5 2)
P54	(9 -2 -2), (9 -2 -1), (9 -1 -2), (9 -1 -1), (9 0 -2), (9 0 -1), (9 1 -2), (9 1 -1), (9 2 -2), (9 2 -1), (10 3 -2), (10 3 -1), (10 4 -2), (10 4 -1), (10 4 0), (10 5 -1), (10 5 0)
P55	(9 -1 -3), (9 0 -4), (9 0 -3), (9 1 -4), (9 1 -3), (9 2 -4), (9 2 -3), (9 3 -4), (9 3 -3), (10 4 -4), (10 4 -3), (10 5 -3), (10 5 -2), (11 6 -3), (11 6 -2)
P56	(9 1 -5), (9 2 -6), (9 2 -5), (9 3 -6), (9 3 -5), (10 4 -5), (10 5 -6), (10 5 -5), (10 5 -4), (11 6 -4)
P57	(10 -4 1), (10 -4 2), (10 -3 1), (10 -3 2), (10 -2 1), (10 -2 2), (10 -1 1), (10 -1 2), (10 0 1), (10 0 2), (10 1 1), (10 1 2), (10 1 3), (11 2 1), (11 2 2), (11 2 3), (11 3 2), (11 3 3), (11 4 2), (11 4 3)
P58	(10 -4 3), (10 -3 3), (10 -2 3), (10 -1 3), (10 0 3), (10 0 4), (10 1 4), (11 2 4), (11 3 4), (11 4 4)

P59	(10 -3 0), (10 -2 -1), (10 -2 0), (10 -1 -1), (10 -1 0), (10 0 -1), (10 0 0), (10 1 -1), (10 1 0), (10 2 -1), (11 2 0), (11 3 -1), (11 3 0), (11 3 1), (11 4 0), (11 4 1), (11 5 0)
P60	(10 -2 -2), (10 -1 -3), (10 -1 -2), (10 0 -3), (10 0 -2), (10 1 -3), (10 1 -2), (10 2 -3), (10 2 -2), (10 3 -3), (11 3 -3), (11 3 -2), (11 4 -3), (11 4 -2), (11 4 -1), (11 5 -2), (11 5 -1)
P61	(10 0 -4), (10 1 -5), (10 1 -4), (10 2 -5), (10 2 -4), (10 3 -5), (10 3 -4), (11 4 -4), (11 5 -5), (11 5 -4), (11 5 -3)
P62	(10 2 -6), (10 3 -6), (10 4 -6), (11 6 -5)
P63	(10 6 -6)
P64	(11 -5 4), (11 -4 3), (11 -4 4), (11 -3 3), (11 -3 4), (11 -2 3), (11 -2 4), (11 -1 3), (11 -1 4), (11 0 3), (11 0 4), (11 1 3), (11 1 4), (12 2 3), (12 2 4), (12 3 4)
P65	(11 -4 1), (11 -4 2), (11 -3 1), (11 -3 2), (11 -2 1), (11 -2 2), (11 -1 1), (11 -1 2), (11 0 1), (11 0 2), (11 1 1), (11 1 2), (12 2 1), (12 2 2), (12 3 1), (12 3 2), (12 3 3), (12 4 2)
P66	(11 -3 -1), (11 -3 0), (11 -2 -1), (11 -2 0), (11 -1 -1), (11 -1 0), (11 0 -1), (11 0 0), (11 1 -1), (11 1 0), (11 2 -1), (12 2 0), (12 3 -1), (12 3 0), (12 4 -1), (12 4 0), (12 4 1)
P67	(11 -2 -2), (11 -1 -3), (11 -1 -2), (11 0 -3), (11 0 -2), (11 1 -3), (11 1 -2), (11 2 -3), (11 2 -2), (12 3 -3), (12 3 -2), (12 4 -3), (12 4 -2), (12 5 -2)
P68	(11 0 -5), (11 0 -4), (11 1 -5), (11 1 -4), (11 2 -5), (11 2 -4), (11 3 -5), (11 3 -4), (11 4 -5), (12 4 -4), (12 5 -4), (12 5 -3), (12 6 -4)
P69	(12 -5 3), (12 -5 4), (12 -4 3), (12 -4 4), (12 -3 3), (12 -3 4), (12 -2 3), (12 -2 4), (12 -1 3), (12 -1 4), (12 0 3), (12 0 4), (12 1 3), (12 1 4), (13 1 5), (13 2 3), (13 2 4), (13 2 5)
P70	(12 -4 1), (12 -4 2), (12 -3 1), (12 -3 2), (12 -2 1), (12 -2 2), (12 -1 1), (12 -1 2), (12 0 1), (12 0 2), (12 1 1), (12 1 2), (13 2 1), (13 2 2), (13 3 1), (13 3 2), (13 3 3)
P71	(12 -3 -1), (12 -3 0), (12 -2 -1), (12 -2 0), (12 -1 -1), (12 -1 0), (12 0 -1), (12 0 0), (12 1 -1), (12 1 0), (12 2 -1), (13 2 -1), (13 2 0), (13 3 -1), (13 3 0), (13 4 -1)
P72	(12 -2 -3), (12 -2 -2), (12 -1 -3), (12 -1 -2), (12 0 -3), (12 0 -2), (12 1 -3), (12 1 -2), (12 2 -3), (12 2 -2), (13 3 -3), (13 3 -2), (13 4 -3), (13 4 -2)
P73	(12 -1 -4), (12 0 -5), (12 0 -4), (12 1 -5), (12 1 -4), (12 2 -5), (12 2 -4), (12 3 -5), (12 3 -4), (13 4 -4), (13 5 -4)
P74	(13 -5 2), (13 -5 3), (13 -4 2), (13 -4 3), (13 -3 2), (13 -3 3), (13 -2 2), (13 -2 3), (13 -1 2), (13 -1 3), (13 0 2), (13 0 3), (13 1 2), (13 1 3), (13 1 4), (14 2 2), (14 2 3), (14 2 4)
P75	(13 -5 4), (13 -4 4), (13 -3 4), (13 -2 4), (13 -1 4), (13 0 4), (14 1 4), (14 1 5)
P76	(13 -4 0), (13 -4 1), (13 -3 0), (13 -3 1), (13 -2 0), (13 -2 1), (13 -1 0), (13 -1 1), (13 0 0), (13 0 1), (13 1 0), (13 1 1), (14 2 0), (14 2 1)
P77	(13 -3 -1), (13 -2 -2), (13 -2 -1), (13 -1 -2), (13 -1 -1), (13 0 -2), (13 0 -1), (13 1 -2), (13 1 -1), (13 2 -2), (14 3 -2), (14 3 -1)
P78	(13 -2 -3), (13 -1 -4), (13 -1 -3), (13 0 -4), (13 0 -3), (13 1 -4), (13 1 -3), (13 2 -4), (13 2 -3), (13 3 -4), (14 3 -3), (14 4 -3)
P79	(14 -5 2), (14 -5 3), (14 -4 2), (14 -4 3), (14 -3 2), (14 -3 3), (14 -2 2), (14 -2 3), (14 -1 2), (14 -1 3), (14 0 2), (14 0 3), (14 1 2), (14 1 3), (15 1 4)
P80	(14 -5 4), (14 -5 5), (14 -4 4), (14 -4 5), (14 -3 4), (14 -3 5), (14 -2 4), (14 -2 5), (14 -1 4), (14 -1 5), (14 0 4), (14 0 5), (15 1 5)
P81	(14 -4 0), (14 -4 1), (14 -3 0), (14 -3 1), (14 -2 0), (14 -2 1), (14 -1 0), (14 -1 1), (14 0 0), (14 0 1), (14 1 0), (14 1 1), (15 2 0)
P82	(14 -3 -2), (14 -3 -1), (14 -2 -2), (14 -2 -1), (14 -1 -2), (14 -1 -1), (14 0 -2), (14 0 -1), (14 1 -2), (14 1 -1), (14 2 -2), (14 2 -1)
P83	(14 -2 -3), (14 -1 -3), (14 0 -3), (14 1 -3), (14 2 -3), (15 3 -3)
P84	(15 -6 4), (15 -6 5), (15 -5 4), (15 -5 5), (15 -4 4), (15 -4 5), (15 -3 4), (15 -3 5), (15 -2 4), (15 -2 5), (15 -1 4), (15 -1 5), (15 0 4), (15 0 5)
P85	(15 -5 1), (15 -5 2), (15 -4 1), (15 -4 2), (15 -3 1), (15 -3 2) (15 -2 1), (15 -2 2), (15 -1 1), (15 -1 2), (15 0 1), (15 0 2), (15 1 1), (15 1 2)
P86	(15 -5 3), (15 -4 3), (15 -3 3), (15 -2 3), (15 -1 3), (15 0 3), (15 1 3)
P87	(15 -4 -1), (15 -4 0), (15 -3 -1), (15 -3 0), (15 -2 -1), (15 -2 0), (15 -1 -1), (15 -1 0), (15 0 -1), (15 0 0), (15 1 -1), (15 1 0), (15 2 -1)
P88	(15 -3 -2), (15 -2 -3), (15 -2 -2), (15 -1 -3), (15 -1 -2), (15 0 -3), (15 0 -2), (15 1 -3), (15 1 -2), (15 2 -3), (15 2 -2)
P89	(16 -6 3), (16 -6 4), (16 -5 3), (16 -5 4), (16 -4 3), (16 -4 4), (16 -3 3), (16 -3 4), (16 -2 3), (16 -2 4), (16 -1 3), (16 -1 4), (16 0 3), (16 0 4), (16 0 5)
P90	(16 -6 5), (16 -5 5), (16 -4 5), (16 -3 5), (16 -2 5), (16 -1 5)

P91	(16 -5 1), (16 -5 2), (16 -4 1), (16 -4 2), (16 -3 1), (16 -3 2), (16 -2 1), (16 -2 2), (16 -1 1), (16 -1 2), (16 0 1), (16 0 2), (16 1 1)
P92	(16 -4 -1), (16 -4 0), (16 -3 -1), (16 -3 0), (16 -2 -1), (16 -2 0), (16 -1 -1), (16 -1 0), (16 0 -1), (16 0 0), (16 1 -1), (16 1 0)
P93	(16 -3 -2), (16 -2 -2), (16 -1 -2), (16 0 -2), (16 1 -2), (16 2 -2)
P94	(17 -6 3), (17 -6 4), (17 -5 3), (17 -5 4), (17 -4 3), (17 -4 4), (17 -3 3), (17 -3 4), (17 -2 3), (17 -2 4), (17 -1 3), (17 -1 4)
P95	(17 -6 5), (17 -5 5), (17 -4 5), (17 -4 6), (17 -3 5), (17 -3 6), (17 -2 5), (17 -2 6), (17 -1 5), (17 -1 6)
P96	(17 -5 1), (17 -5 2), (17 -4 1), (17 -4 2), (17 -3 1), (17 -3 2), (17 -2 1), (17 -2 2), (17 -1 1), (17 -1 2), (17 0 1), (17 0 2)
P97	(17 -4 -1), (17 -4 0), (17 -3 -1), (17 -3 0), (17 -2 -1), (17 -2 0), (17 -1 -1), (17 -1 0), (17 0 -1), (17 0 0), (17 1 -1)
P98	(17 -3 -2), (17 -2 -2), (17 -1 -2)
P99	(18 -4 1), (18 -4 2), (18 -3 1), (18 -3 2), (18 -2 1), (18 -2 2), (18 -1 1), (18 -1 2)
P100	(18 -4 3), (18 -4 4), (18 -3 3), (18 -3 4), (18 -2 3), (18 -2 4), (18 -1 3)
P101	(18 -4 5), (18 -4 6), (18 -3 5), (18 -3 6), (18 -2 5), (18 -2 6)
P102	(18 -3 -1), (18 -3 0), (18 -2 -1), (18 -2 0), (18 -1 -1), (18 -1 0), (18 0 -1), (18 0 0)
P103	(19 -2 4), (19 -2 5)
P104	(19 -1 0), (19 -1 1)

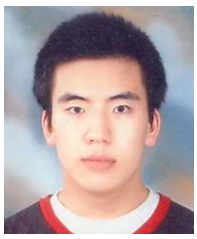

Keuyhong Cho received his BSc in Physics from Sejong University, Seoul, Korea, in 2015. He is currently a Master's student in the Vision & Image Processing Laboratory at Sejong University. His research interest is image processing.

Jusun Lee received his BSc in Computer Engineering from Sejong University, Seoul, Korea, in 2015. He is currently a Master's student in the Vision & Image Processing Laboratory at Sejong University. His research interest is image processing.

Sanghoon Song received his BSc in Electronics Engineering from Yonsei University, Seoul, Korea, in 1977, and an MSc in 1979 from the Department of Computer Science, KAIST, Korea. He received his PhD in 1992 from the Department of Computer Science at the University of Minnesota, Minneapolis, U.S.A. Since 1992, he has been with the Department of Computer Engineering, Sejong University, Korea, where he is currently a professor. His research interests are embedded computing systems, computer arithmetic, and distributed systems.

Dongil Han received his BSc in Computer Engineering from Korea University, Seoul, Korea, in 1988 and an MSc in 1990 from the Department of Electric and Electronic Engineering, KAIST, Daejeon, Korea. He received his PhD in 1995 from the Department of Electric and Electronic Engineering at KAIST, Daejeon, Korea. From 1995 to 2003, he was Senior Researcher in the Digital TV Lab of LG Electronics. Since 2003, he has been with the Department of Computer Engineering, Sejong University, Korea, where he is currently a professor. His research interests include image processing.